Experimental evaluation of a radiation dose management system-integrated 3D skin dose map by comparison with XR-RV3 Gafchromic® films

Joël Greffier, Nicolas Grussenmeyer-Mary, Ahmed Larbi, Jean Goupil, Guillaume Cayla, Bertrand Ledermann, Jean Paul Beregi, Julien Frandon

▶ **To cite this version:**

Joël Greffier, Nicolas Grussenmeyer-Mary, Ahmed Larbi, Jean Goupil, Guillaume Cayla, et al.. Experimental evaluation of a radiation dose management system-integrated 3D skin dose map by comparison with XR-RV3 Gafchromic® films. Physica Medica, 2019, 66, pp.77-87. 10.1016/j.ejmp.2019.09.234 . hal-02794426

HAL Id: hal-02794426
https://hal.umontpellier.fr/hal-02794426

Submitted on 20 Jul 2022

HAL is a multi-disciplinary open access archive for the deposit and dissemination of scientific research documents, whether they are published or not. The documents may come from teaching and research institutions in France or abroad, or from public or private research centers.

L'archive ouverte pluridisciplinaire **HAL**, est destinée au dépôt et à la diffusion de documents scientifiques de niveau recherche, publiés ou non, émanant des établissements d'enseignement et de recherche français ou étrangers, des laboratoires publics ou privés.

Distributed under a Creative Commons Attribution - NonCommercial 4.0 International License

Version of Record: https://www.sciencedirect.com/science/article/pii/S1120179719304417
Manuscript_be4484576176e2bfa2aa077f91cca21b

Experimental evaluation of a radiation dose management system-integrated 3D skin dose map by comparison with XR-RV3 Gafchromic® films.

J. Greffier[1,*], N. Grussenmeyer-Mary[2], A. Larbi[1], J. Goupil[1], G. Cayla[3], B. Ledermann[3], J.P. Beregi[1], J. Frandon[1].

1. Service d'imagerie medicale, CHU Nimes, Univ Montpellier, Medical Imaging Group Nimes, EA 2415, Nimes, France

2. GE Healthcare, DoseWatch, R&D, Strasbourg, France

3. Service de cardiologie, CHU Nimes, Univ Montpellier, Medical Imaging Group Nimes, EA 2415, Nimes, France

* Corresponding author: Joël Greffier, CHU de Nîmes, Medical Imaging Group Nîmes, EA 2415, Bd Prof Robert Debré, 30029 Nîmes Cedex 9; tel: +33.466.683.309; fax: +33.466.683.308; mail: joel.greffier@chu-nimes.fr

© 2019 published by Elsevier. This manuscript is made available under the CC BY NC user license
https://creativecommons.org/licenses/by-nc/4.0/

Abstract

Objective

To assess the interactive Skin Dose Map® tool (SDM_{Tool}) integrated to the Radiation Dose Management System (RDMS) DoseWatch with Gafchromic films for implementation in routine practice.

Methods

A retrospective dose estimation software SDM_{Tool} was used to calculate peak skin dose (PSD) and display the patient skin dose distribution. PSD was calculated with a triangle mesh of 0.055cm² resolution on ICRP 110 male anthropomorphic phantom and with a square ROI of 1cm² on flat phantom. The tool uses Radiation Dose Structured Reports (RDSR) data to model exposure events and calculate the PSD per event. The PSD and the skin dose distribution estimated with SDM_{Tool} were evaluated in comparison with Gafchromic films positioned under the PMMA phantom (20cm) for 13 configurations. Measurements were performed on a Philips system. Statistical analysis were carried out to compare PSD_{Film} and PSD_{SDM}.

Results

Average differences between PSD_{Film} and PSD_{SDM} were 6%±6% (range from -3% to 22%) for flat phantom and 5%±7% (range from -3% to 25%) for ICRP phantom. Concordance was good between the measured PSD_{Film} and the estimated PSD_{SDM} with Lin's coefficient estimation and 95% Confidence Interval of 0.979[0.875; 0.984] for flat phantom and 0.977[0.877; 0.985] for ICRP phantom. Dose map representations are concordant for 11 of the 13 tests on PMMA phantom. Disparities arose from the limitations of the RSDR format: table displacement during fluoroscopy events and the use of wedge filter.

Conclusion

The results found in this experimental evaluation show that the SDM_{Tool} is a suitable alternative to Gafchromic® film to calculate PSD.

Keywords:

Radiation physics; Fluoroscopy; Experimental; Dosimetry; Physics; Radiation safety; Dosimetric comparison.

Abbreviation:

PSD: Peak skin dose

RDMS: Radiation dose management system

SDM: Skin dose map

RDSR: Radiation dose structured reports

Introduction

Interventional radiology and cardiology procedures are of great diagnostic and therapeutic benefit [1; 2]. However, during long and complex procedures, the skin doses delivered to the patient can be high and exceed the thresholds for deterministic effects (skin dose > 2Gy) [3-7]. In these cases, it may be necessary to perform a Peak Skin Dose (PSD) assessment in order to locate the maximum skin dose delivered to the patient and improve their therapeutic follow-up.

PSD assessment is usually complex and time-consuming. Several direct measurement systems of PSD exist, including radiochromic films [8-13]. These large-size films provide a dose map at the end of the procedure where film darkening is proportional to the dose delivered to the patient's skin. However, these films are expensive and have many constraints to their routine use (such as long and tedious calibration, correct positioning of the film, and specific storage conditions) [8; 13].

Commercial systems are available to evaluate PSD during the procedure (Dose Tracking System (Canon Medical systems, Tokyo, Japan) [14], Dose Map (GE Healthcare, Milwaukee, USA) [15; 16] or *a posteriori* (em.dose (esprimed)) [8; 17]. These systems calculate the PSD using the dosimetric and technical information recorded during the procedure. Recently, skin dose estimation algorithms have been integrated into radiation dose management system (RDMS) such as Radiation Dose Monitor (Medsquare, Paris, France), Radimetrics^{TM} (Bayer Healthcare, Whippany, USA) and DOSE (Qaelum, Leuven, Belgique). The aim of these tools is to provide a retrospective assessment of PSD value and a dose map, independent of the make and model of the imaging system. A common requirement is that the DICOM radiation dose structured report (RDSR) is sent to the RDMS, containing dose indices, acquisition information, and beam and table geometry.

There is little data in the literature concerning the validation of PSD and skin dose map distributions for these software applications. The few studies available have some limitations in the comparative assessment as defined by Habib Geryes *et al.*[18]. In their study, the authors compared the PSDs and the 2D dose distributions calculated by the

Radiation Dose Monitor tool (Medsquare, Paris, France) and measured with Gafchromic® XR-RV3 films. This precise and complete phantom study was performed on two interventional radiology systems for 17 different configurations (simple and complex).

The purpose of this study is to compare the PSD and skin dose map distribution as measured with XR-RV3 Gafchromic® films and estimated with the interactive Skin Dose Map® tool (SDM_{Tool}) integrated the RDMS DoseWatch® (GE Healthcare, Milwaukee, USA). This phantom study was performed on an interventional radiology system for 13 different exposure configurations.

Materials and methods

Skin Dose Map (SDM) calculation formalism

The RDMS DoseWatch® includes the estimation of skin dose as part of its core dose management capabilities. The interactive Skin Dose Map® tool (SDM_{Tool}) is integrated in the RDMS DoseWatch®. At the end of the procedure, each interventional imaging system transfers the RDSR data to DoseWatch® RDMS. RDSR data include dosimetric (such as kVp, additional filtration, Air Kerma, Kerma Area Product) and geometric (such as primary and secondary angulation, table position) information for each event of fluoroscopy and fluorography. SDM_{Tool} uses RDSR data to calculate the PSD per event following recommendations defined by K. Jones *et al.*[12]:

$$Peak\ Skin\ Dose = RPAK\ \times \frac{SRPD^2}{d_{Skin}^2} \times CF \times BF \times AF_{Skin} \times AF_{Table} \quad (1)$$

The Reference Point Air Kerma (**RPAK**) provided by the equipment for each event is the cumulative air kerma at the interventional reference point (IRP) located 15 cm back from isocenter towards the focal spot of an interventional imaging system. The Source to Reference Point Distance (**SRPD**) is defined by the manufacturer for each system and corresponds to the distance between the source and the IRP.

Correction factors (**CF**) are used to correct the difference between the RPAK provided by the equipment and RPAK measured in-house by a qualified physicist. Usually, the medical physicist defines CF per equipment and for fluoroscopy and fluorography events from a reproducible protocol. The tolerance accepted for CF by the AAPM Imaging Physics Committee Task Group 190 is ± 35% [19].

The distance from source to patient skin ($\mathbf{d_{Skin}}$) is computed by SDM_{Tool} in two steps based on RDSR data. First, the SDM_{Tool} uses information from DICOM tags (standard or private): "Table Height Position", "Height of System", “Table Longitudinal Position”, “Table Lateral Position”, “Positioner Primary Angle”, “Positioner Secondary Angle” and (SOD) to compute the distance from source to table (d_{Table}):

$$d_{Table} = Table\ height\ position + SOD - Height\ of\ system \quad (2)$$

"Table Height Position", “Table Longitudinal Position” and “Table Lateral Position” correspond respectively to the vertical, longitudinal and lateral table position for each event. “Positioner Primary Angle” and “Positioner Secondary Angle” correspond to the primary angulation (Left Anterior Oblique and Right Anterior Oblique) and the secondary angulation (Cranial-Caudal) for each event. "Height of system" and “Source Object Distance (SOD)” are fixed for each system.

Second, an average compressed mattress thickness is added to d_{Table} to model the mattress placed between the table and the patient’s back. This value was defined especially for this study by measuring the average thickness of the compressed mattress on 20 patients of different morphologies.

For each event, SDM_{Tool} defines a Half-Value Layer (HVL) based on kVp and filtrations (inherent and additional) used. The HVL values are calculated beforehand with the Spekcalc software (McGill University, Montreal, Canada) by taking into account the inherent and additional filtrations and kVp available in the system used. Once the beam quality is determined based on the HVLs, the backscatter factor (**BF**), the skin absorption factor ($\mathbf{AF_{Skin}}$) and the mattress and table attenuation factor ($\mathbf{AF_{Table}}$) are determined based on look-up tables in the software.

The backscatter factor (**BF)** is computed using available data in Table 1 of the ICRU report 74 [20] as function of kVp, HVL and equivalent-square field sizes. When present in the DICOM file, the collimated field area on the detector is used. Otherwise, and when present in the DICOM file, private tags such as Philips Shutters positions are used to compute the collimated field area at a known distance from the source. Otherwise, the collimated field area at the reference point is approximated by dividing the KAP by the RPAK. Then, field size at the patient entrance position (d_{Skin}) is computed by applying inverse square law.

The skin absorption factor ($\mathbf{AF_{Skin}}$), corresponding to the skin-to-air mass energy absorption coefficients, is defined following the composition of soft tissues for children or adults available in Table 13.2 of ICRP report 89 [21] combined with the elemental values of National Institute of Standards and Technology (NIST) [22]. For each HVL, mass energy

absorption coefficients for air $(\mu_{en}/\rho)_{air}$ and skin $(\mu_{en}/\rho)_{Skin}$ are computed. AF_{Skin} corresponds to the ratio $\left[\frac{\mu en}{\rho}\right]_{air}^{Skin}$ for a given HVL.

The table attenuation factor (**AF_{Table}**) includes table and mattress attenuations as follows: $AF_{Table} = e^{-\mu_{Table\ and\ Matress} \times d_{Table\ and\ Mattress}}$.

A ray-tracing algorithm [16; 23; 24] computes the table and mattress thicknesses for each event using the primary angulation, the secondary angulation and the d_{Skin} reported in the RSDR. Since the composition of the table and/or the mattress tend to be proprietary by manufacturers, the $\mu_{Table\ and\ Mattress}$ cannot be computed directly. Based on the published works from DeLorenzo *et al.*[25], a nominal equivalent table and mattress thickness in aluminum of 1.4mm was used. The equivalent thickness of table and mattress ($d_{Table\ and\ Mattress}$) in aluminum, traversed by the x-ray beam, is then calculated for each incidence. The aluminum attenuation coefficient of table and mattress ($\mu_{Table\ and\ Mattress}$) is computed from the elemental values of NIST [22] based on calculated HVL for each incidence.

The different parameters used for the calculation of PSD by the SDM_{Tool} are presented in Table 1.

Skin Dose Map (SDM) patient representation and dose reporting

DoseWatch® uses two types of phantom to estimate the dose: flat (2D) and the adult male or female ICRP (3D).

The flat phantom represents a simplified geometry not intended for real patient events. This flat phantom was designed to perform dosimetry validation studies, typically using Gafchromic® films, in an easier and more accurate way. It is modeled as a flat surface of 0.055 cm² triangles laying on top of the mattress and spanning the patient table. The PSD was computed in a ROI of 1 cm² to mimic the reading methodology of Gafchromic® films.

The ICRP reference male and reference female phantoms are based on the voxelated phantom representations provided by ICRP 110 [26]. Both phantoms are available

in DoseWatch® and the same methodology using a mesh of triangles is used to generate their 3D shapes. The average area per triangle is 0.055 cm².

DoseWatch® extracts all irradiation event information from the DICOM Radiation Dose Structured Report object (RDSR). It automatically choses the appropriate 3D phantom based on the patient's sex. The table and mattress are modeled as a flat surface. The table position is determined using the information available in the RDSR (table height, table longitudinal and lateral position, table head tilt, table tilt). The beam is represented as a pyramid, the focal spot being the summit, the surface on the detector being the base. However, the RDSR does not provide, in a standard way, any information regarding the shape of the beam, which is generally assumed to be square. For some devices though, the information is available in vendor-specific private tags that DoseWatch® extracts from the RDSR. For the Philips system used during this work, the information is provided through the position of the shutters DICOM Tag "99PHI-IXR-XPER/005". The beam position is determined using various data fields in the RDSR (left/right and cranial/caudal angulations, C-arm position). The phantom is positioned on top of the table. The software rotates the phantom, if needed, to consider the patient position provided in the RDSR. The patient position relative to the table top has to be manually adjusted as this information is not present in the RDSR; the default setting is 10 cm between the table top edge and the patient's head. The dose information is cumulated on all the irradiation events to provide a comprehensive skin dose map distribution for the whole exam.

DoseWatch® presents the skin dose map distribution as a 3D interactive view that the user can rotate and zoom in or out to focus on relevant body regions (Figure 1). This provides visualization of complex dose distributions potentially resulting from bi-plane systems. The PSD is extracted from the skin dose map distribution, as the maximum dose cumulated on the meshed triangle surface. To better assess the contribution of a single event, a timeline is provided, and the various views of the software updated to display a partial SDM and PSD up to the selected event.

Gafchromic® Film

Reflective XR-RV3 Gafchromic® films (Ashland, Advanced Materials, USA) were used in this study (batch number: 09241802). Films were calibrated free-in-air in an interventional imaging system: Allura Xper FD 20 (Philips Medical Systems, Best, Netherlands) according to the same methodology previously described[27; 28]. Films were placed on a 6 cm-thick expanded polystyrene support providing negligible backscatter and irradiated at 37 cm from the focal spot. A flat ionization chamber 10x6-60 (Radcal, Monrovia, USA) is positioned 1.5 cm above the films at 38.5 cm from the focal spot (Figure 2.a). The inverse square law is applied to correct air Kerma (AK) measurements. In order to have the totality of the ionization chamber in the exposure field, a diagonal of 48 cm without electronic zoom was used. The ionization chamber and its converter are calibrated in a dosimetry laboratory for three different beam qualities: RQR3, RQR5 and RQR9 beams [29]. Films were cut to 7 cm x 8 cm, and placed white side facing source as recommended by the film manufacturer. Each film was exposed individually in the same position of the X-ray field. Films were exposed at seven different dose levels (0, 0.2, 0.5, 1.0, 1.5, 2.0 and 3.0 Gy). Calibration was performed for three different beam qualities (70, 90, 120 kVp and additional filtration of 0.1 mmCu + 1 mmAl) to best represent clinical exposures. The half layer value for each beam quality was equal to 4.29 mm for 70 kVp, 5.37 mm for 90 kVp and 7.03 mm for 120 kVp.

The exposed films were stored in a support in stable conditions of temperature and humidity after the procedure[30; 31]. Films were scanned, orange-side down in the scanner, at 1 week ±1 h post exposure, with an Epson 10,000 Expression XL as per manufacturer recommendations. Each exposed film (7 cm x 8 cm) is scanned individually in the center of the scanner to overcome the non-uniformity of the scanner [27; 32]. The software Film Qa-XR (Ashland, Advanced Materials, USA) was used to analyze film images. A square region of interest (ROI), approximately 2 cm x 2 cm, was placed in the center of each film image. According to the manufacturer recommendations, the red color channel was used[27; 28]. The mean measured reflective density was associated to the measured AK and a calibration curve was obtained.

An uncertainty assessment was performed for the skin dose measurements with XR-RV3 Gafchromic films (Table 2). The relative combined standard uncertainty was estimated at 13.2% (k = 1) and relative expanded uncertainty was 26.4% (k = 2). These estimated uncertainties are in the same range as those observed in previous studies [17; 18; 27; 32; 33].

Comparison of PSD obtained with Gafchromic® film and SDM tool

Dose maps and PSD's obtained with Gafchromic® films were compared against those with DoseWatch® SDM_{Tool} for flat and ICRP phantoms. A PMMA phantom of 30x30 cm² and 20 cm thick was positioned on the table and on the mattress (Figure 2.b). XR-RV3 Gafchromic® films were placed between the mattress and the phantom. Thirteen configurations were evaluated in an interventional imaging system available in our institution. Eleven configurations were performed to compare the independent impact of simple projection, multiple projections, detector to tube distance, patient to tube distance, FOV, collimation (field size), the use of wedge filter and table displacements (in all directions) between fluorography events and during fluoroscopy events. Two configurations were performed to compare the combined impact of previous parameters on skin dose map calculation. The description of the different configurations was presented in Table 3.

The 13 exposed films were read 1 week ±1 h after the exposure, respecting the same process described previously for the film calibration. Based on the beam quality selected by the X-ray system when exposing the PMMA phantom, the 70 kVp calibration curve most closely matched the beam quality for all film exposures. A square ROI of 1 cm² was manually positioned by the medical physicist in the maximum dose region with the software Film Qa-XR®. The average value of this ROI represented the PSD_{Film}. SDM_{Tool} calculates the skin dose for each event from the previously defined calculation formalism. At the end of the calculation, SDM_{Tool} provides the PSD_{SDM} and dose distribution obtained on the flat phantom and the ICRP phantom. For the flat phantom, PSD_{SDM} was computed from a square ROI of 1 cm² to be similar to the measurement of PSD_{Film}.

Statistical Analysis

Statistical analysis was performed using our in-house developed Matlab routine (MathWorks, Natick, USA). The relationship between PSD_{Film} and PSD_{SDM} was evaluated with Lin's concordance correlation coefficient and classified as nonexistent (0.00-0.59), poor (0.60-0.79), acceptable (0.80-0.89), or good (0.90 – 1.00).

Results

Comparison of measured and computed PSD

Table 4 and Figure 3 show the results of the PSD_{Film} and PSD_{SDM} for the flat and ICRP phantoms for the 13 configurations. PSD_{Film} values ranged from 459 to 1027 mGy and PSD_{SDM} values ranged from 471 to 1033 mGy for flat phantom and from 472 to 1028 mGy for ICRP phantom. The average difference between PSD_{Film} and PSD_{SDM} was 6%±6% (range from -3% to 22%) for flat phantom and 5%±7% (range from -3% to 25%) for ICRP phantom.

The concordance between PSD_{Film} and PSD_{SDM} is good (>0.9) according to Lin's concordance correlation coefficient (Figure 4). The Lin's coefficient estimation and 95% CI are 0.979 [0.875; 0.984] for flat phantom and 0.977 [0.877; 0.985] for ICRP phantom.

Comparison of dose maps

The dose maps obtained with SDM_{Tool} are similar to those recorded with the software Film Qa-XR after film assessment. Sizes, shapes and positions of the different exposure fields on the dose maps with SDM_{Tool} are relatively the same to those present on the Gafchromic® films, especially for simple configurations. Figure 5 shows five dose maps obtained with the two softwares for simple configurations (C4, C5, C7, C8, C9) and Figure 6 shows the dose maps obtained for the two combined configurations (C12 and C13).

Variations in dose map representation are observed for two configurations: C10 and C11. Figure 7.a shows that software does not model one-sided and two-sided wedge filters. The PSD being located in the center of the field, this omission does not involve a significant variation of the PSD obtained with the film and the software (10% for both phantoms). Figure 7.b depicts the impact of table displacement during fluoroscopic events. Indeed, the DICOM RSDR gives the geometric positions of the tube and the table only for the last fluoroscopy image and therefore does not take into account any table or tube displacements during a fluoroscopic event. This has the effect of overestimating the PSD calculated with both phantoms (22% for flat and 25% for ICRP).

Discussion

Accurate PSD assessment is notoriously complex and so the use of Gafchromic® films remains the reference method. As RDMS become more established, integrated skin dose calculation tools not only facilitate skin dose assessment but also make it more accessible to users (such as medical physicists or physicians). To our knowledge, these tools are available and marketed in several RDMS: Radimetrics (Bayer) Radiation Dose Monitor (Medsquare), DOSE (Qaelum) and DoseWatch (GE Healthcare). For the first time, this phantom study compares experimentally the PSD estimated with the SDM_{Tool} integrated to the DoseWatch® RDMS to the ones measured with Gafchromic® films for 13 configurations on a Philips interventional imaging system.

The outcomes of this study show a good correlation between the PSD values measured with the Gafchromic® films and those estimated with SDM_{Tool} for the for both phantom selections. The obtained results are in the same range as those obtained with other software and available in the literature [8; 14-18; 34]. Using Dose Map, Bordier *et al*. found a difference of 25.0% on an anthropomorphic phantom and 14.3% on one patient for a complex fenestrated aortic endovascular repair [15; 16]. Two teams compared em.dose: Magnier *et al*. found an average difference of 4.7% on anthropomorphic phantom and a median difference of 8.5% over 59 thoracic or abdominopelvic endovascular interventions[17]; and Greffier *et al*. found a difference of 3.4% ± 21.1% (method A) and 17.3% ± 23.9% (method B) on 40 patients who received coronary angiography and coronary angioplasty for one or two vessels disease or complex coronary angioplasty of chronic total occlusion [8]. The variation between these two studies is due to the different calculation methodologies. Magnier *et al*. [17] used the fluoroscopy and fluorography information available in the RSDR, whereas in the study by Greffier *et al*. [8], the PSD computation was carried out based on the DICOM information available on the PACS for the fluorography events. To factor for the contribution of the fluoroscopy on PSD, two methods were used: either equal spread over all digital cine event series (method A) or cumulated at the position of the most exposing cine event (method B). Regarding Dose Tracking System® (Canon

Medical systems, Tokyo, Japan), Rana *et al.* found a <4% difference for the SK150 head phantom [14]. However, in this study, the Gafchromic® films were not calibrated free-in-air but in contact with a PMMA phantom accounting for backscattered radiation. Finally, using the Radiation Dose Monitor tool, Habib Geryes *et al.* [18] found an average difference of 10%±7% for a Siemens Artis Zee and 9%±7% for GE Innova IGS interventional systems. This robust and comprehensive study carried out on phantoms for 17 configurations is the most appropriate for comparison. Indeed, the methodology used in our study was modeled on that described by Habib Geryes *et al.* [18]. However, our study is carried out with 13 configurations on the same system. It should also be noted that in the present study, the PSD is calculated on both 2D flat phantom and 3D ICRP phantom whereas in the Habib Geryes study [18] it is only calculated on a flat 2D phantom with the Radiation Dose Monitor software.

The results of this study also show that the obtained dose maps with SDM_{Tool} are relatively similar to those obtained from the Gafchromic® films. Indeed, the shapes, sizes and positions of the beams are concordant. However, variations in dose maps are observed for two configurations (C-10 and C-11). For the C-10 configuration, the software doesn't model the wedge filters used during fluoroscopy and fluorography events. This is due to lack of information in the RDSR. The software assigns the same skin dose value to the entire exposed field because no information on the use of wedge filters is available in the RDSR. This has no impact on the PSD calculated in this phantom study because there is no change of tube angulation or table movement for this configuration. However, in patients this could lead to overlapped areas of field not present on the film, increasing the calculated PSD by the software. In clinical practice, these wedge filters are very often used in interventional cardiology procedures to correct the attenuation difference between the lung and the heart. For the configuration C-11, for each fluoroscopy event, the software will place the exposure field based on the last position of the table and tube. Indeed, the software is limited by the geometrical information present in the RSDR, which does not contain data on manipulation of the table and the tube throughout the fluoroscopy events. In our study, this leads to the

addition of two overexposure zones not present on the film, resulting in a 25% increase in the value of PSD on the ICRP phantom. On a patient, this could cause variations of the PSD calculated in either direction according to the variations of positioning of the tube and the table between the events of fluoroscopy and fluorography. In addition, this will especially impact procedures where the proportion of fluoroscopy is high compared to fluorography (such as complex coronary angioplasty of chronic total occlusion).

As with any software, SDM_{Tool} has differentiators and limitations. First, the results of this study show that this tool can accurately calculate the PSD for simple and combined configurations. PSD can be calculated for all patients tracked in the system. PSD values are computed automatically without additional manual action, are easily accessible from the RDMS, but are not provided with calculation uncertainties. Limitations of the SDM_{Tool} are not due to algorithm gaps but from data gaps in the RDSR. Upon connection of a new system to the RDMS, the reliability of RDSR data generated by the system needs to be assessed. As with Radiation Dose Monitor, the PSD is obtained retrospectively but much faster than with Gafchromic® films or software like em.dose. In addition, the PSD is not obtained in real time as with Dose Tracking System® or Dose Map® during the procedure.

Second, this tool calculates the PSD on an anthropomorphic 3D ICRP phantom, which makes it possible to improve the distribution of the dose according to the anatomical zone, the incidence and the positioning of the table. However, only two phantoms are currently available, and it is necessary to increase the phantom library to account for differences in patient morphology (impacting the dose distribution). To our knowledge, with the exception of Radimetrics® using 15 phantoms, all other available systems for calculating the PSD offline use a single 2D phantom.

Third, the exposure fields are positioned on the 3D phantom based on the table information (up / down, right / left) available in the RDSR and this positioning does not always reflect the actual patient's position, resulting in the dose being attributed to the wrong skin location. This point is very important, especially for cumulative PSD evaluation during iterative procedures on the same anatomical area. To better reflect the reality and cover the

right anatomical region, it is possible to modify case by case in the SDM_{Tool} the "distance between the top of the table and the head of the patient". However, the lateral position of the patient on the table cannot be adapted; the tool assumes that the patient is centered. Using a positioning camera existing in some CT scan might further improve the accuracy of cumulative PSD and skin dose maps. It should be noted that this problem is common to all solutions.

Fourth, the SDM_{Tool} is able to reproduce rectangular fields through the use of private fields available in the RDSR. This is not currently available via Radiation Dose Monitor. This improves the precision of the dose map representations and the calculated PSD values. Finally, like Radiation Dose Monitor, the SDM_{Tool} is an interactive tool able to replay each fluoroscopic and fluorographic event by projecting them onto the phantom. This is an educational tool making the operator (interventional radiologist or cardiologist) aware of the impact of operator-dependent parameters (such as collimation, electronic zoom, frame rate, variations in the incidence of tube-patient and patient-detector distances) on the PSD and the dose map.

This study presents some limitations. First, Gafchromic® films are used as the gold standard in this study, however their precision is close to ± 20% [17; 18; 27; 32; 33]. Second, this study is done for a single manufacturer available in our institution and without rotational events. A similar study should be performed to assess the reproducibility of the results on the other systems and with rotational events. Third, this experimental study is performed on a PMMA phantom with uniform density, which is relatively far from the patient density. A study on patients should be performed to assess the reproducibility of the results for interventional cardiology and other fluoroscopically guided procedures. Finally, as defined by Habib Geryes *et al.* [18], a gamma index analysis between the obtained dose maps with the films and with SDM_{Tool} could not be performed because of the lack of suitable software.

Conclusion

This experimental evaluation demonstrates that this RDMS-integrated 3D Skin Dose Map is a suitable alternative to the use of Gafchromic® film, which can be complex, time

consuming, and expensive to use, especially when the film technique fails due to positioning, or processing errors. Differences between dose maps and PSDs measured with the film technique and those calculated with SDM_{Tool} are acceptable considering the uncertainties associated with the use of Gafchromic® films. A study on patients should be performed to assess the reproducibility of the results found in this study for interventional cardiology and vascular procedures.

Acknowledgements

We thank C. Steinville, D. Miller and S. Kabani for their help in editing the manuscript. We thank P.A. Daviau and C. Demattei for their support in this study.

Disclosure of Conflicts of Interest

N. Grussenmeyer-Mary works for the GE Healthcare company. All the other authors have no relevant conflicts of interest to disclose.

References

1 Hamm CW, Bassand JP, Agewall S et al (2011) ESC Guidelines for the management of acute coronary syndromes in patients presenting without persistent ST-segment elevation: The Task Force for the management of acute coronary syndromes (ACS) in patients presenting without persistent ST-segment elevation of the European Society of Cardiology (ESC). Eur Heart J 32:2999-3054

2 Silber S, Albertsson P, Aviles FF et al (2005) [Guidelines for percutaneous coronary interventions]. Rev Esp Cardiol 58:679-728

3 Balter S, Hopewell JW, Miller DL, Wagner LK, Zelefsky MJ (2010) Fluoroscopically guided interventional procedures: a review of radiation effects on patients' skin and hair. Radiology 254:326-341

4 Koenig TR, Wolff D, Mettler FA, Wagner LK (2001) Skin injuries from fluoroscopically guided procedures: part 1, characteristics of radiation injury. AJR Am J Roentgenol 177:3-11

5 Miller DL, Balter S, Cole PE et al (2003) Radiation doses in interventional radiology procedures: the RAD-IR study: part II: skin dose. J Vasc Interv Radiol 14:977-990

6 Shope TB (1996) Radiation-induced skin injuries from fluoroscopy. Radiographics 16:1195-1199

7 Vano E, Goicolea J, Galvan C et al (2001) Skin radiation injuries in patients following repeated coronary angioplasty procedures. Br J Radiol 74:1023-1031

8 Greffier J, Van Ngoc Ty C, Bonniaud G et al (2017) Assessment of peak skin dose in interventional cardiology: A comparison between Gafchromic film and dosimetric software em.dose. Phys Med 38:16-22

9 Greffier J, Moliner G, Pereira F et al (2017) Assessment of Patient's Peak Skin Dose Using Gafchromic Films During Interventional Cardiology Procedures: Routine Experience Feedback. Radiat Prot Dosimetry 174:395-405

10 Ying CK, Kandaiya S (2010) Patient skin dose measurements during coronary interventional procedures using Gafchromic film. J Radiol Prot 30:585-596

11 Jones AK, Ensor JE, Pasciak AS (2014) How accurately can the peak skin dose in fluoroscopy be determined using indirect dose metrics? Med Phys 41:071913

12 Jones AK, Pasciak AS (2011) Calculating the peak skin dose resulting from fluoroscopically guided interventions. Part I: Methods. J Appl Clin Med Phys 12:3670

13 Greffier J, Goupil J, Larbi A et al (2018) Assessment of patient's peak skin dose during abdominopelvic embolization using radiochromic (Gafchromic) films. Diagn Interv Imaging 99:321-329

14 Rana VK, Rudin S, Bednarek DR (2013) Updates in the real-time Dose Tracking System (DTS) to improve the accuracy in calculating the radiation dose to the patients skin during fluoroscopic procedures. Proc SPIE Int Soc Opt Eng 8668:86683Z

15 Bordier C, Klausz R, Desponds L (2015) Accuracy of a dose map method assessed in clinical and anthropomorphic phantom situations using Gafchromic films. Radiat Prot Dosimetry 165:244-249

16 Bordier C, Klausz R, Desponds L (2015) Patient dose map indications on interventional X-ray systems and validation with Gafchromic XR-RV3 film. Radiat Prot Dosimetry 163:306-318

17 Magnier F, Poulin M, Van Ngoc Ty C et al (2018) Comparison of Patient Skin Dose Evaluated Using Radiochromic Film and Dose Calculation Software. Cardiovasc Intervent Radiol 41:762-771

18 Habib Geryes B, Hadid-Beurrier L, Waryn MJ, Jean-Pierre A, Farah J (2018) Benchmarking the DACS-integrated Radiation Dose Monitor(R) skin dose mapping software using XR-RV3 Gafchromic(R) films. Med Phys 45:4683-4692

19 Lin PJ, Schueler BA, Balter S et al (2015) Accuracy and calibration of integrated radiation output indicators in diagnostic radiology: A report of the AAPM Imaging Physics Committee Task Group 190. Med Phys 42:6815-6829

20 ICRU Report 74. Patient Dosimetry for X Rays used in Medical Imaging (Report 74). 2005.

21 ICRP Publication 89. Basic Anatomical and Physiological Data for Use in Radiological Protection: Reference Values. 2002.

22 Hubbell JH SS (1995) Tables of X-Ray Mass Attenuation Coefficients and Mass Energy-Absorption Coefficients 1 keV to 20 MeV for Elements Z = 1 to 92 and 48 Additional Substances of Dosimetric Interest. NIST

23 Johnson PB, Borrego D, Balter S, Johnson K, Siragusa D, Bolch WE (2011) Skin dose mapping for fluoroscopically guided interventions. Med Phys 38:5490-5499

24 Khodadadegan Y, Zhang M, Pavlicek W et al (2011) Automatic monitoring of localized skin dose with fluoroscopic and interventional procedures. J Digit Imaging 24:626-639

25 DeLorenzo MC, Yang K, Li X, Liu B (2018) Comprehensive evaluation of broad-beam transmission of patient supports from three fluoroscopy-guided interventional systems. Med Phys 45:1425-1432

26 Menzel HG, Clement C, DeLuca P (2009) ICRP Publication 110. Realistic reference phantoms: an ICRP/ICRU joint effort. A report of adult reference computational phantoms. Ann ICRP 39:1-164

27 McCabe BP, Speidel MA, Pike TL, Van Lysel MS (2011) Calibration of GafChromic XR-RV3 radiochromic film for skin dose measurement using standardized x-ray spectra and a commercial flatbed scanner. Med Phys 38:1919-1930

28 Greffier J, Van Ngoc Ty C, Agelou M et al (2016) Impact of the calibration conditions of XR-RV3 films on peak skin dose measurements in interventional radiology. Radiat Prot Dosimetry. 10.1093/rpd/ncw116

29 IEC 61267. Medical Diagnostic X-ray Equipment - Radiation Conditions for Use in the 463 Determination of Characteristics. 2005.

30 Niroomand-Rad A, Blackwell CR, Coursey BM et al (1998) Radiochromic film dosimetry: recommendations of AAPM Radiation Therapy Committee Task Group 55. American Association of Physicists in Medicine. Med Phys 25:2093-2115

31 Delle Canne S, Carosi A, Bufacchi A et al (2006) Use of GAFCHROMIC XR type R films for skin-dose measurements in interventional radiology: Validation of a dosimetric procedure on a sample of patients undergone interventional cardiology. Phys Med 22:105-110

32 Farah J, Trianni A, Ciraj-Bjelac O et al (2015) Characterization of XR-RV3 GafChromic((R)) films in standard laboratory and in clinical conditions and means to evaluate uncertainties and reduce errors. Med Phys 42:4211-4226

33 Farah J, Trianni A, Carinou E et al (2015) Measurement of maximum skin dose in interventional radiology and cardiology and challenges in the set-up of European alert thresholds. Radiat Prot Dosimetry 164:138-142

34 Bednarek DR, Barbarits J, Rana VK, Nagaraja SP, Josan MS, Rudin S (2011) Verification of the performance accuracy of a real-time skin-dose tracking system for interventional fluoroscopic procedures. Proc SPIE Int Soc Opt Eng 7961

Figure legends

Figure 1. Screen shot of DoseWatch® Skin Dose Map tool.

Figure 2. a. Free-in-air calibration of XR-RV3 Gafchromic films; b. Exposure conditions of XR-RV3 Gafchromic films using PMMA phantom for PSD assessment

Figure 3. Comparison of PSD values for the 13 configurations assessed on the Allura Xper FD10. Error bars were defined to 20% of the PSD values measured by XR-RV3 Gafchromic® films.

Figure 4. Lin's concordance correlation between measured and calculated PSD.

Figure 5. FilmQA-XR dose maps versus SDM_{Tool} maps obtained with flat and ICRP phantoms for simple configurations: C-4 (a), C-5 (b), C-7 (c), C-8 (d) and C-9 (e).

Figure 6. FilmQA-XR dose maps versus SDM_{Tool} maps obtained with flat and ICRP phantoms for combined configurations: C-12 (a) and C-13 (b).

Figure 7. FilmQA-XR maps versus SDM_{Tool} maps obtained with flat and ICRP phantoms for configurations: C-10 (a) and C-11 (b).

Series Information

Run number	Start time	Protocol serie	Acquisition mode	Auto exposure preference	Frame rate	FOV	DAP serie (mGy.cm²)	RPAK serie (mGy)	Peak Skin Dose serie (mGy)	Irradiation time serie (s)	Patient orientation
1	08:42:43	1 Cardiac Faible dose DYNAMIC	RECORD STATIONARY_ACQUISITION	ROI +	15.2627	17.2	32.5	51.39	40.13	3.21045	HFS

a.
b.

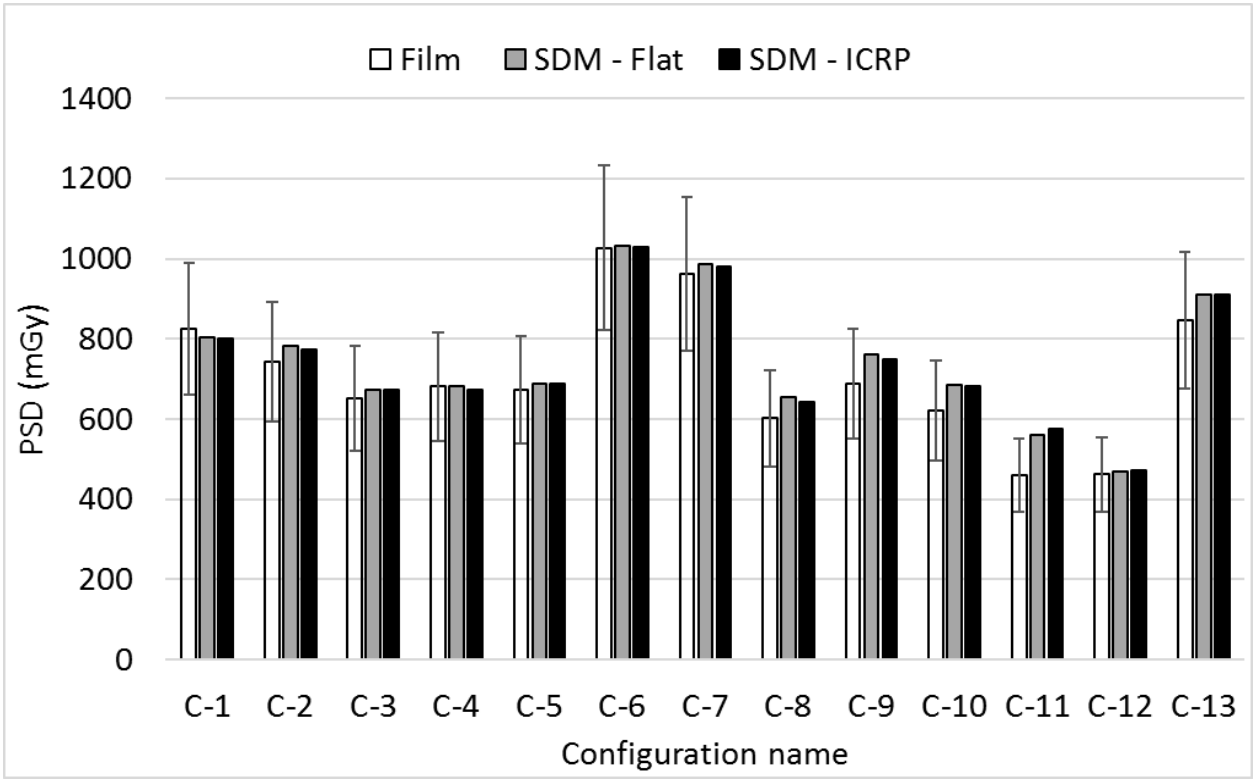
Film
SDM - Flat
SDM - ICRP
1400
1200
1000
800
600
400
200
0
PSD (mGy)
C-1
C-2
C-3
C-4
C-5
C-6
C-7
C-8
C-9
C-10
C-11
C-12
C-13
Configuration name

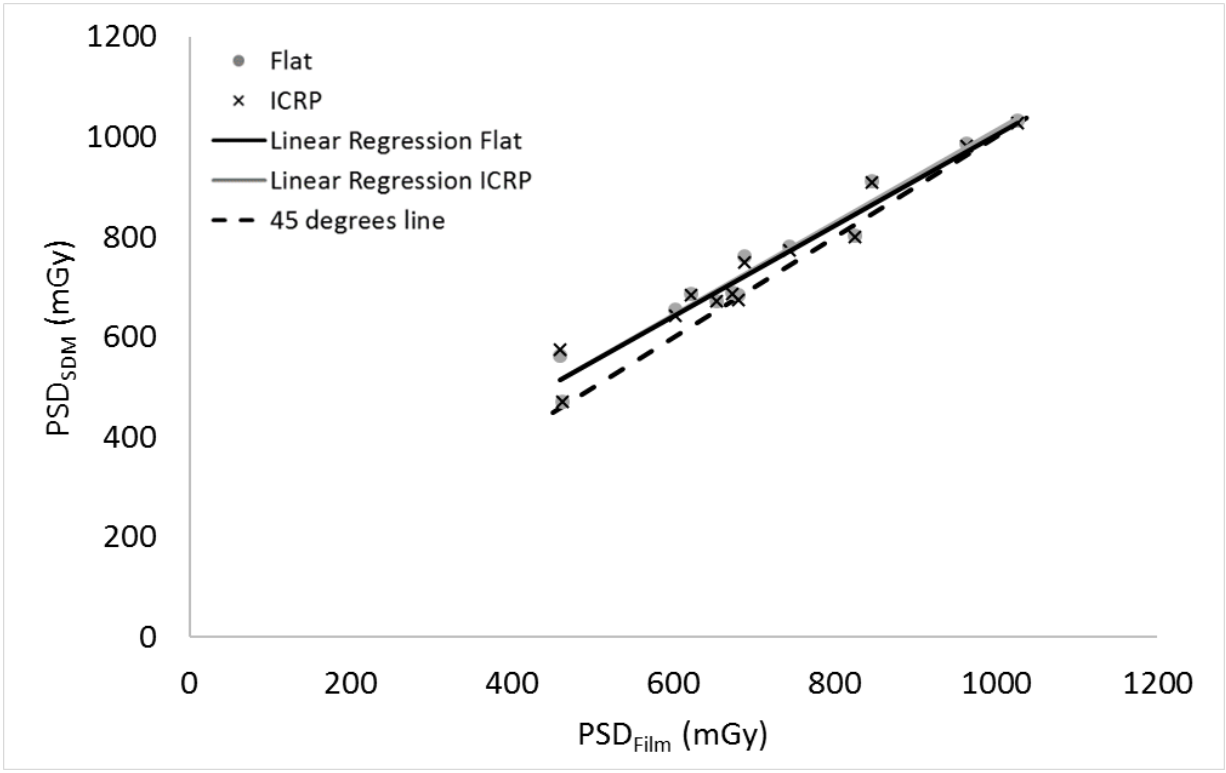
1200
1000
800
600
400
200
0
0
200
400
600
800
1000
1200
Flat
ICRP
Linear Regression Flat
Linear Regression ICRP
45 degrees line
PSDSDM (mGy)
PSDFilm (mGy)

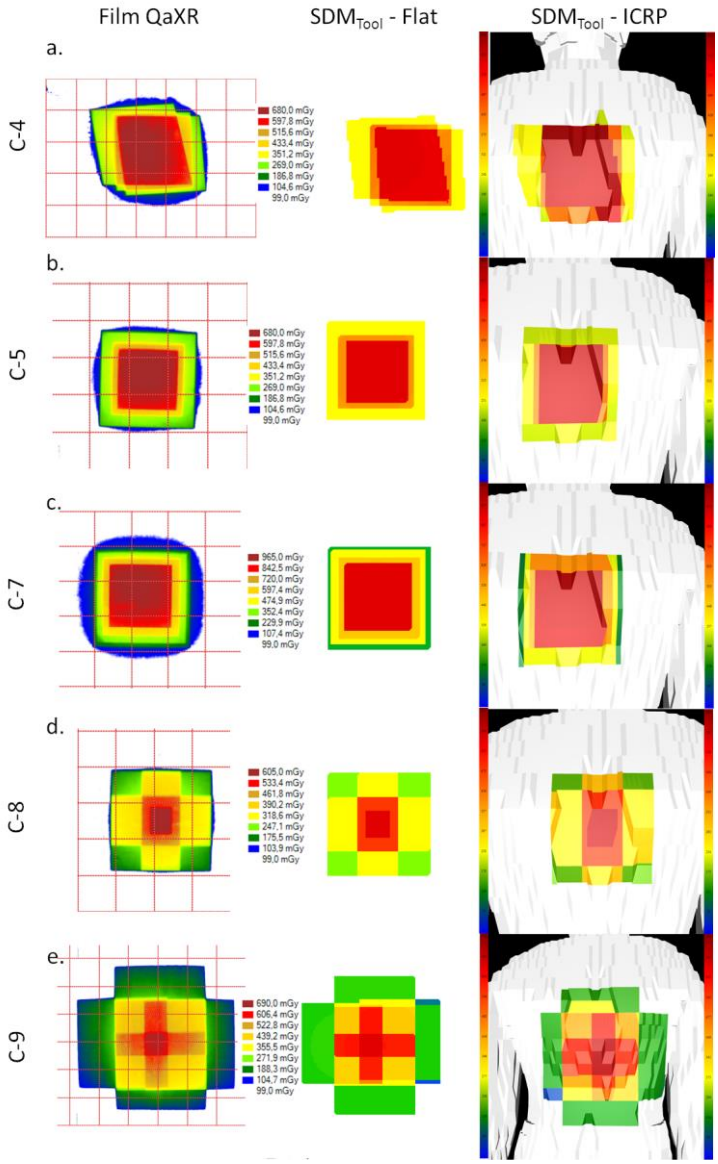
Film QaXR
SDM$_{Tool}$ - Flat
SDM$_{Tool}$ - ICRP
a.
C-4
680,0 mGy
597,8 mGy
515,6 mGy
433,4 mGy
351,2 mGy
269,0 mGy
186,8 mGy
104,6 mGy
99,0 mGy
b.
C-5
680,0 mGy
597,8 mGy
515,6 mGy
433,4 mGy
351,2 mGy
269,0 mGy
186,8 mGy
104,6 mGy
99,0 mGy
c.
C-7
965,0 mGy
842,5 mGy
720,0 mGy
597,4 mGy
474,9 mGy
352,4 mGy
229,9 mGy
107,4 mGy
99,0 mGy
d.
C-8
605,0 mGy
533,4 mGy
461,8 mGy
390,2 mGy
318,6 mGy
247,1 mGy
175,5 mGy
103,9 mGy
99,0 mGy
e.
C-9
690,0 mGy
606,4 mGy
522,8 mGy
439,2 mGy
355,5 mGy
271,9 mGy
188,3 mGy
104,7 mGy
99,0 mGy

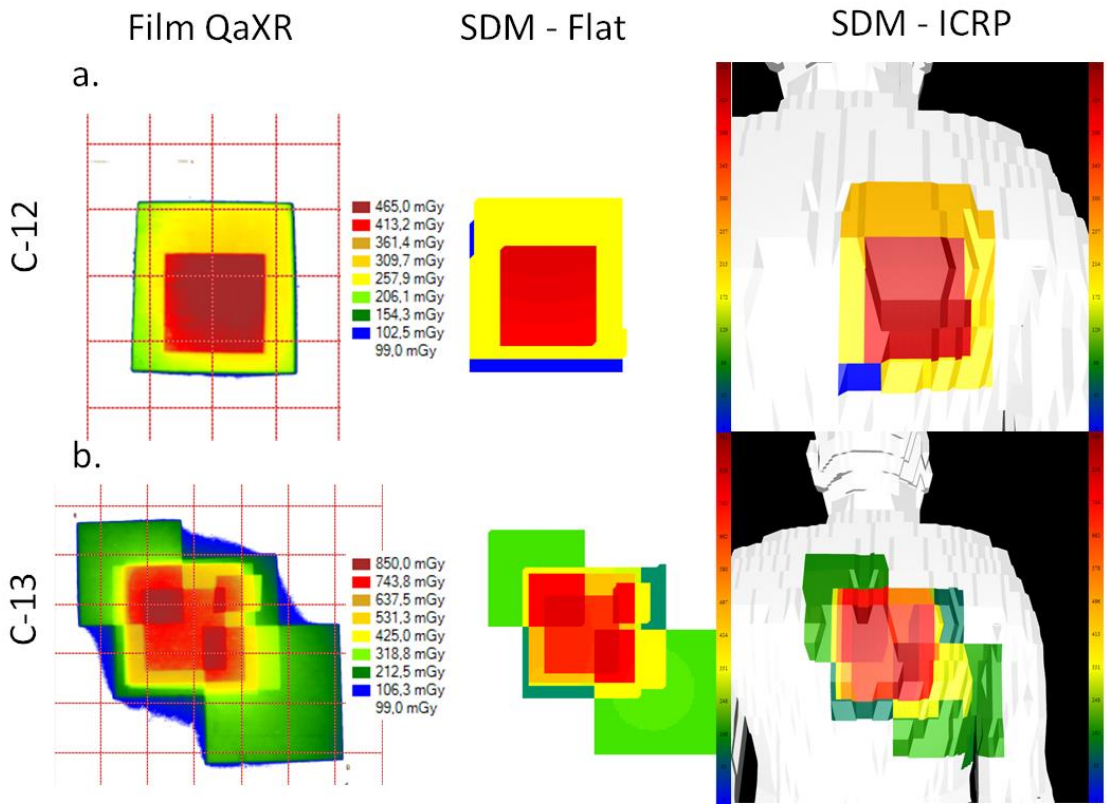
Film QaXR
SDM - Flat
SDM - ICRP
a.
C-12
465,0 mGy
413,2 mGy
361,4 mGy
309,7 mGy
257,9 mGy
206,1 mGy
154,3 mGy
102,5 mGy
99,0 mGy
b.
C-13
850,0 mGy
743,8 mGy
637,5 mGy
531,3 mGy
425,0 mGy
318,8 mGy
212,5 mGy
106,3 mGy
99,0 mGy

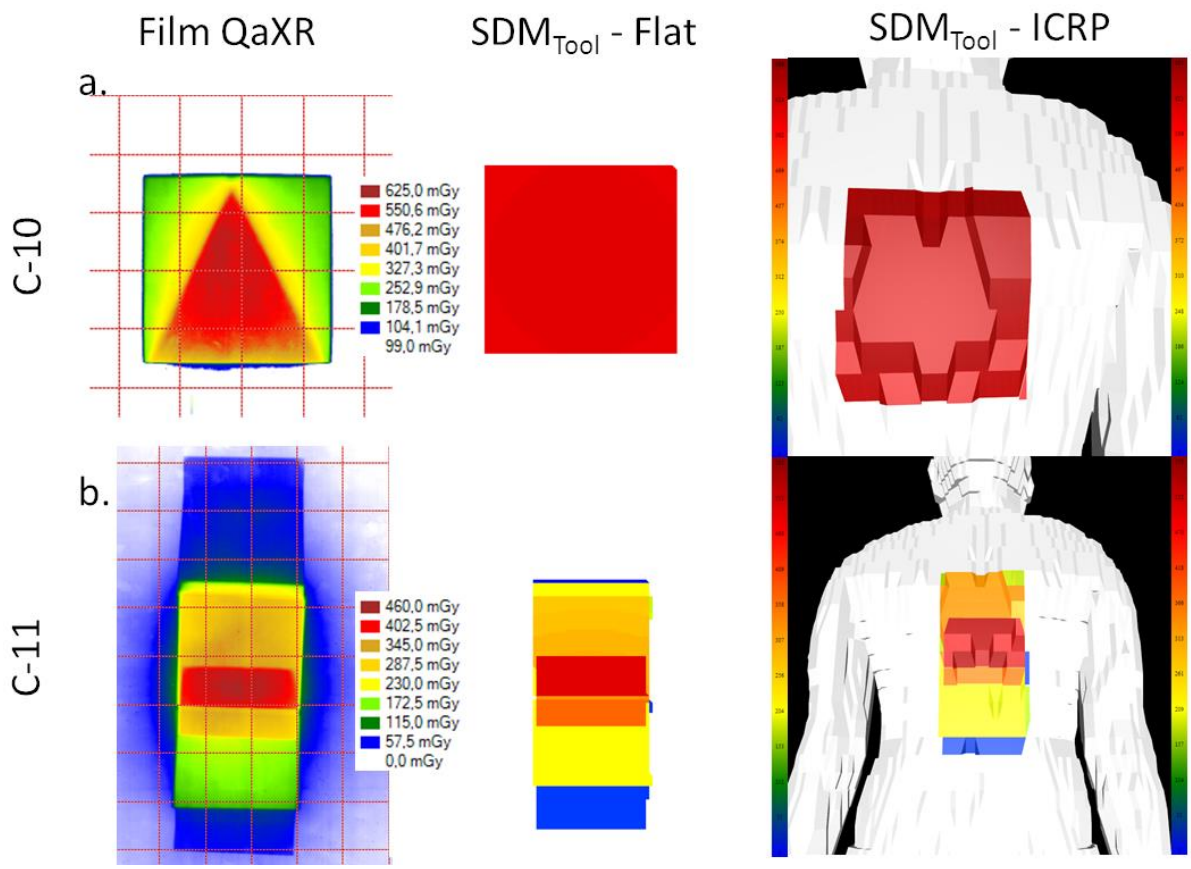
Film QaXR
SDM$_{Tool}$ - Flat
SDM$_{Tool}$ - ICRP
a.
C-10
625,0 mGy
550,6 mGy
476,2 mGy
401,7 mGy
327,3 mGy
252,9 mGy
178,5 mGy
104,1 mGy
99,0 mGy
b.
C-11
460,0 mGy
402,5 mGy
345,0 mGy
287,5 mGy
230,0 mGy
172,5 mGy
115,0 mGy
57,5 mGy
0,0 mGy

Table 1. Parameters available used for the calculation of the PSD by the SDM_{Tool} on the system assessed.

Model	Allura Xper FD10
SRPD (cm)	61.5
SOD (cm)	76.5
Thickness of the uncompressed mattress (cm)	7
Average compressed mattress thickness (cm)	4
CF fluorography	0.986
CF fluoroscopy	1.020
Inherent filtration	3 mmAl
Additional filtration	0.1 mmCu + 1 mmAl
	0.4 mmCu + 1 mmAl
	0.9 mmCu + 1 mmAl
kVp range	From 50 to 125

Table 2. Uncertainty assessment for the skin dose measurements with XR-RV3 Gafchromic films

Source of uncertainty	Type of uncertainty	Value (%)	Comments
Scanner uncertainty	Scan uniformity	0.5	Measured on our scanner (Epson 10000XL)
	Pixel value uncertainty within ROI	1.3	
Dose measurement uncertainty	Ionization chamber (10X6-60) measurements	1.2	Calibration certificate
	Beam uniformity	1.6	Measured on our system (Philips Allura Xper FD 20)
Film and calibration uncertainties	Film-to-film uniformity in one batch	2.5	McCabe et al. [27]
	Dose rate dependence	3.0	Farah et al. [32]
	Radiation quality dependence	2.0	Farah et al. [32]
	Calibration (fitting equation…)	12.0	Farah et al. [32]

Table 3. Description of the 13 configurations assessed on the interventional radiology equipment and used to compare PSD and dose maps using XR-RV3 Gafchromic® films and SDM_{Tool}.

Configuration parameters	Configuration number	Type of events	kV	mAs	KAP (mGy.cm²)	AK (mGy)	Field size at SRPD (cm²)	Tube projection	Tube-detector distance (cm)	Tube entrance distance (cm)	Add Filtration	Table Height	FOV (cm)	Collimation	Table displacement	Wedge filter
Simple projection and events	1	Low fluoroscopy (15f/s)	89	8.6	3400	36	94	PA	120	69	0.4 + 1	10	25	No	No	No
		Mean Fluoroscopy (15f/s)	79	19.7	6804	73	94	PA	120	69	0.4 + 1	10	25	No	No	No
		High Fluoroscopy (15f/s)	75	15.2	10161	109	94	PA	120	69	0.1 + 1	10	25	No	No	No
		Fluorography (30f/s)	73	4.2	87431	930	94	PA	120	69	0.1 + 1	10	25	No	No	No
Influence of multiple projections	2	Fluorography (30f/s)	73	4.2	47285	509	93	PA	120	69	0.1 + 1	10	25	No	No	No
		Fluorography (30f/s)	78	5.8	45296	491	92	RAO 30	120	69	0.1 + 1	10	25	No	No	No
	3	Fluorography (30f/s)	73	4.2	28617	310	92	PA	120	69	0.1 + 1	10	25	No	No	No
		Fluorography (30f/s)	78	5.8	29048	310	94	RAO 30	120	69	0.1 + 1	10	25	No	No	No
		Fluorography (30f/s)	81	5.5	27115	294	92	RAO 45	120	69	0.1 + 1	10	25	No	No	No
	4	Fluorography (30f/s)	73	4.2	28189	304	93	PA	120	69	0.1 + 1	10	25	No	No	No
		Fluorography (30f/s)	75	4.8	28302	300	94	LAO 20; CRAN 10	120	69	0.1 + 1	10	25	No	No	No
		Fluorography (30f/s)	80	5.6	28199	303	93	RAO 30; CAUD 15	120	69	0.1 + 1	10	25	No	No	No
Influence of FOV	5	Fluorography (30f/s)	73	4.2	28241	306	92	PA	120	69	0.1 + 1	10	25	No	No	No
		Fluorography (30f/s)	75	4.8	15514	293	52	PA	120	69	0.1 + 1	10	20	No	No	No
		Fluorography (30f/s)	78	5.8	11172	304	37	PA	120	69	0.1 + 1	10	15	No	No	No
Influence of tube detector distance	6	Fluorography (30f/s)	73	4.3	23436	253	93	PA	120	59	0.1 + 1	0	25	No	No	No
		Fluorography (30f/s)	72	3.9	26861	246	109	PA	110	59	0.1 + 1	0	25	No	No	No
		Fluorography (30f/s)	70	2.9	32692	254	129	PA	100	59	0.1 + 1	0	25	No	No	No
		Fluorography (30f/s)	69	2.6	39298	250	157	PA	90	59	0.1 + 1	0	25	No	No	No
Influence of tube entrance distance	7	Fluorography (30f/s)	73	4.3	23147	254	91	PA	121	48	0.1 + 1	-11	25	No	No	No
		Fluorography (30f/s)	73	4.2	22401	249	90	PA	121	59	0.1 + 1	0	25	No	No	No
		Fluorography (30f/s)	73	4.2	22327	252	89	PA	121	69	0.1 + 1	10	25	No	No	No
		Fluorography (30f/s)	73	4.1	22211	249	89	PA	121	75	0.1 + 1	16	25	No	No	No
Influence of collimation	8	Fluorography (30f/s)	73	4.2	22734	253	90	PA	121	75	0.1 + 1	16	25	No	No	No
		Fluorography (30f/s)	73	4.3	11259	250	45	PA	121	75	0.1 + 1	16	25	Lat	No	No

		Fluorography (30f/s)	73	4.3	9740	283	34	PA	121	75	0.1 + 1	16	25	Long	No	No
		Fluorography (30f/s)	97	5.3	1170	229	5	PA	121	75	0.1 + 1	16	25	Both	No	No
Influence of table displacement between fluorography events	9	Fluorography (30f/s)	70	2.81	27503	204	135	PA	100	69	0.1 + 1	10	25	No	No	No
		Fluorography (30f/s)	70	2.82	27879	206	135	PA	100	69	0.1 + 1	10	25	No	Foot	No
		Fluorography (30f/s)	70	2.83	26626	198	134	PA	100	69	0.1 + 1	10	25	No	Head	No
		Fluorography (30f/s)	70	2.81	27207	203	134	PA	100	69	0.1 + 1	10	25	No	Left	No
		Fluorography (30f/s)	70	2.8	26688	199	134	PA	100	69	0.1 + 1	10	25	No	Right	No
Influence of wedge filter	10	Fluorography (30f/s)	70	2.9	25477	255	100	PA	100	69	0.1 + 1	10	25	No	No	Right
		Fluorography (30f/s)	70	2.9	26228	248	106	PA	100	69	0.1 + 1	10	25	No	No	Left
		Fluorography (30f/s)	70	2.9	28767	394	73	PA	100	69	0.1 + 1	10	25	No	No	Right/Left
Influence of table displacement during fluoroscopy events	11	Fluorography (30f/s)	73	4.2	22933	243	95	PA	100	69	0.1 + 1	10	25	No	No	No
		Fluorography (30f/s)	78	5.8	19688	211	94	CRAN 30	100	69	0.1 + 1	10	25	No	No	No
		Low fluoroscopy (7.5f/s)	87	10.5	4231	47	90	CRAN 30	100	69	0.1 + 1	10	25	No	Yes	No
		Fluorography (30f/s)	68	2.4	17150	187	92	CAUD 30	100	69	0.1 + 1	10	25	No	No	No
		Low fluoroscopy (7.5f/s)	81	10.5	5800	64	91	CAUD 30	100	69	0.1 + 1	10	25	No	Yes	No
Combined influence of multiple projections and FOV	12	Fluorography (30f/s)	78	5.8	11277	310	36	PA	120	69	0.1 + 1	10	15	No	No	No
		Fluorography (30f/s)	75	4.7	27145	303	90	CAUD 20	120	69	0.1 + 1	10	25	No	No	No
Combined influence of tube detector distance. tube detector entrance. FOV. collimation and table displacement	13	Fluorography (30f/s)	73	4.2	16867	186	91	PA	120	69	0.1 + 1	10	25	No	No	No
		Fluorography (30f/s)	74	5.9	19826	219	91	RAO 30	120	75	0.1 + 1	16	25	No	No	No
		Fluorography (30f/s)	70	2.9	18068	201	90	PA	100	69	0.1 + 1	10	25	No	No	No
		Fluorography (30f/s)	71	3.8	19935	201	99	CAUD 10	110	75	0.1 + 1	16	25	No	No	No
		Fluorography (30f/s)	76	5.1	8392	201	42	CRAN 10	110	69	0.1 + 1	10	15	No	No	No
		Fluorography (30f/s)	76	5.9	2936	203	14	LAO 20; CAUD 10	100	59	0.1 + 1	0	20	Middle Lat/Long	No	No
		Fluorography (30f/s)	69	2.7	17964	195	92	PA	90	59	0.1 + 1	0	25	Strong Lat/Long	Head/Right	No
		Fluorography (30f/s)	69	2.6	17784	200	89	PA	90	59	0.1 + 1	0	20	No	Foot/Left	No

Table 4. Peak Skin Dose measured with XR-RV3 Gafchromic® films and computed by SDM_{Tool} for each configuration.

Configuration	Peak Skin Dose (mGy)		
	Film	SDM_{Tool} - Flat	SDM_{Tool} - ICRP
C-1	825	803	800
C-2	744	781	774
C-3	653	672	672
C-4	681	683	674
C-5	674	689	687
C-6	1027	1033	1028
C-7	963	986	981
C-8	602	654	643
C-9	688	762	749
C-10	622	686	683
C-11	459	562	575
C-12	463	471	472
C-13	846	910	909